We are IntechOpen,
the world's leading publisher of
Open Access books
Built by scientists, for scientists

4,800
Open access books available

122,000
International authors and editors

135M
Downloads

Our authors are among the

154
Countries delivered to

TOP 1%
most cited scientists

12.2%
Contributors from top 500 universities

CLARIVATE ANALYTICS
BOOK CITATION INDEX
INDEXED

WEB OF SCIENCE™

Selection of our books indexed in the Book Citation Index
in Web of Science™ Core Collection (BKCI)

Interested in publishing with us?
Contact book.department@intechopen.com

Numbers displayed above are based on latest data collected.
For more information visit www.intechopen.com

Preparation and Electrochemical Properties of Cathode and Anode Materials for Lithium Ion Battery by Aerosol Process

Takashi Ogihara
University of Fukui,
Japan

1. Introduction

Lithium ion battery (LIB) has been used as energy storage devices for portable electronics since 1990 years. Recently, these are well noted as the power sources for the vehicles such as electric vehicles and hybrid electric vehicles. Both layered type $LiCoO_2$, $LiNiO_2$ and spinel type $LiMn_2O_4$ is the most important cathode materials because of their high operating voltage at 4 V (Mizushima, et.al, 1980, Guyomard, et.al, 1994). So far, $LiCoO_2$ has been mostly used as cathode material of commercial LIB. However, $LiCoO_2$ and $LiNiO_2$ have a problem related to capacity fading due to the instability in rechargeable process. Cobalt is also expensive and its resource is not sufficient. Therefore, $LiCoO_2$ cathode material is not suitable as a LIB for EV and HEV. On the other hand, $LiMn_2O_4$ is regarded as a promising cathode material for large type LIB due to their advantages such as low cost, non-toxicity and thermally stability (Pegeng, et.al, 2006). It was also known that Ni-substitute type $LiMn_2O_4$ ($LiNi_{0.5}Mn_{1.5}O_4$) was exhibited rechargeable behavior at about 5 V (Markovsky, et.al, 2004, Idemoto, et.al, 2004, Park, et.al, 2004). $LiNi_{0.5}Mn_{1.5}O_4$ has been considerably noticed as a cathode material with high power density which had an active potential at 5 V. The layered type $LiCo_{1/3}Ni_{1/3}Mn_{1/3}O_2$ was found to exhibit superior high potential cathode properties. This had rechargeable capacity with more than 150 mAh/g at higher rate and a milder thermal stability, but shows significantly capacity fading during the long rechargeable process. Recently, olivine type phosphate compound is noted as an alternative cathode material. $LiFePO_4$ and $LiMnPO_4$ were expected as next generation materials for large LIB because of low-cost, environmentally friendly, high thermally stability and electrochemical performance. On the other hand, the oxide type anode such as spinel type $Li_4Ti_5O_{12}$ is expected as the candidate for the replacement of carbon anodes because of better safety. LIB which is consisted of $LiFePO_4$ cathode and $Li_4Ti_5O_{12}$ anode offers to high safety and long life cycle. Therefore, it is expected as the application of HEV or power supply for load levelling in wind power generation and solar power generation. So far, we have been developed spray pyrolysis technique as a aerosol process to prepare $LiFePO_4$ and $Li_4Ti_5O_{12}$ powders for LIB. In this chapter, the powder processing and electrochemical properties of $LiFePO_4$ cathode and $Li_4Ti_5O_{12}$ anode materials by spray pyrolysis were described.

2. Spray pyrolysis process

Spray pyrolysis is a versatile process regarding the powder synthesis of inorganic and metal materials (Messing, et.al, 1993, Dubois, et.al, 1989, Pluym, et.al, 1993). An atomizer such as ultrasonic (Ishizawa, et.al, 1985) or two-fluid nozzle (Roy, et.al, 1977) is often used to generate the mist. The mist is droplet in which the inorganic salts or metal organic compound is dissolved in water or organic solvent. The droplets were dried and pyrolyzed to form oxide or metal powders at elevated temperature. The advantages of spray pyrolysis are that the control of particle size, particle size distribution and morphology are possible. Furthermore, the fine powders with homogeneous composition can be easily obtained because the component of starting solution is kept in the mist derived from an ultrasonic atomizer or two-fluid nozzle. Each metal ion was homogeneously blending in each mist. Each mist play a role as the chemical reactor at the microscale. The production time was very short (less than 1 min). In the other solution process such sol-gel, hydrothermal, precipitation, hydrolysis, the oxide powders were often prepared for few hours. In addition, the process such as the separation, the drying and the firing step must be done after the chemical reaction in the solution. The oxide powders are continuously obtained without these steps in the spray pyrolysis. So far, it has been reported that this process is effective in the multicomponent oxide powders such as $BaTiO_3$ (Ogihara, et.al, 1999) and alloy powders such as Ag-Pd (Iida, et.al, 2001). Recently, layered type of lithium transition metal oxides such as $LiCoO_2$ (Ogihara, et.al 1993), $LiNiO_2$ (Ogihara, et.al, 1998), $LiNi_{0.5}Mn_{1.5}O_4$ (Park, et.al, 2004), $LiNi_{1/3}Mn_{1/3}Co_{1/3}O_2$ (Park, et.al, 2004) and spinel type of lithium transition metal oxides such as $LiMn_2O_4$ (Aikiyo, et.al, 2001), which are used as the cathode materials for Li ion batteries also have been synthesized by spray pyrolysis. It has been clear that these cathode materials derived from spray pyrolysis showed excellent rechargeable performances. This revealed that the particle characteristics such as uniform particle morphology, narrow size distribution and homogeneous chemical composition led to higher rechargeable capacity, higher efficiency, long life cycle and higher thermal stability.

3. LiFePO$_4$/C cathode materials

The electrochemical properties of olivine-type $LiFePO_4$ cathode materials exhibit a relatively high theoretical capacity of 170 mAh/g and a stable cycle performance at high temperatures. However, in the past, the low electrical conductivity of $LiFePO_4$ prevented its application as a cathode material for the lithium-ion battery. Therefore, conductive materials such as carbon and foreign metals were added to $LiFePO_4$ in order to enhance its electrical conductivity (Padhi, et.al, 1997, Bewlay, et.al, 2004, Wang, et.al, 2005, Barker, et.al, 2003). So far, the composite materials of $LiFePO_4$ and carbon have been synthesized by various types of solution techniques such as sol-gel method, hydrothermal thermal, emulsion and spray drying and solid state reaction. On the other hand, the carbon coating on $LiFePO_4$ powders have been also carried out after the preparation of pure $LiFePO_4$ powders. The advantage of spray pyrolysis is that the precursor of $LiFePO_4$/C materials is obtained at one step for very short time. The various types of organic compounds such as white sugar, ascorbic acid and citric acid were used as a carbon source to enhance the electrical conductivity of $LiFePO_4$ in spray pyrolysis.

3.1 Preparation of LiFePO₄/C cathode materials

$LiNO_3$, $Fe(NO_3)_3 \cdot 9H_2O$, and H_3PO_4 were used as starting materials. They were weighted out to attain a molar ratio of Li:Fe:P = 1:1:1 and then dissolved in double distilled water to prepare the aqueous solution. Various types of organic compounds such as sucrose, fructose, sugar or citric acid were added to aqueous solutions up to 60 wt% as carbon source. Figure 1 shows the schematic diagram of the spray pyrolysis apparatus. It consisted of an ultrasonic transducer, electric furnace, and cyclone. The mist of aqueous solution was generated with ultrasonic transducer (2.4 MHz) with 0.08 dm^3/s of air carrier gas. The droplet size (D_P) of mist generated using an ultrasonic transducer were very small and can be determined by equation (1), where ρ is the density of water as a solvent, γ is the surface tension of water, f is the frequency of the transducer. The mist was introduced to the electric furnace. The pyrolysis temperature of electric furnace was 500 °C. As-prepared LiFePO₄/C powders were continuously collected by using the cyclone. As-prepared LiFePO₄/C powders were heat treated at 700 °C for 10 h in the electric furnace under argon (95 %)/hydrogen (5 %) atmosphere.
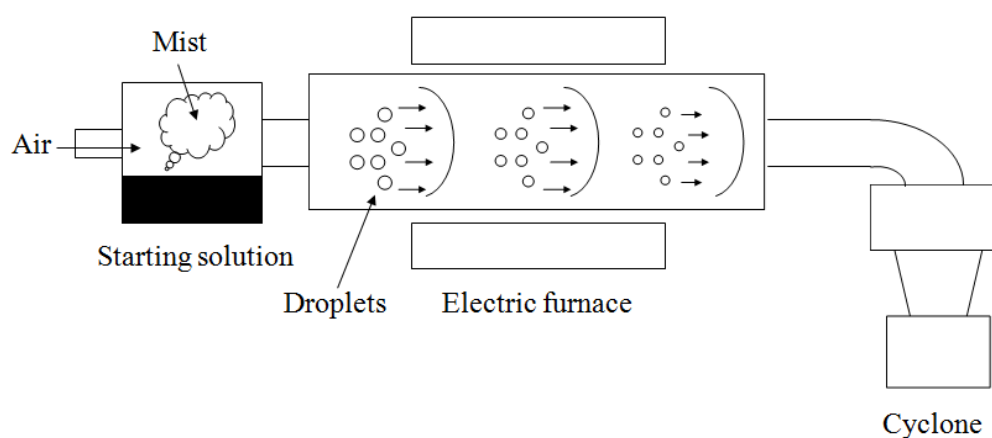

Fig. 1. Schematic diagram of spray pyrolysis with ultrasonic transducer

$$D_p = 0.34 \left(\frac{8\pi\gamma}{\rho f^2} \right)^{1/3} \tag{1}$$

3.2 Particle characterizations of LiFePO₄/C cathode materials

Figure 2 shows SEM photographs of as-prepared LiFePO₄/C powders prepared by spray pyrolysis of an aqueous solution of sucrose and citric acid. The average particle size, morphology, and microstructure of the LiFePO₄/C powders were determined using a scanning electron microscope (SEM). The as-prepared LiFePO₄/C particles had a spherical morphology with a smooth surface and non-aggregation regardless of the type of carbon sources used. Figure 2 also shows that these have hollow particles. This resulted in the drastic decomposition of organic acid in the step of pyrolysis. The average particle sizes of as-prepared LiFePO₄/C powders obtained from sucrose and citric acid were approximately 1 μm. The particle size distribution of LiFePO₄/C powders ranged from 0.2 μm to 3 μm. It was found that these powders had a broad size distribution because of the broad size distribution of the mist generated by the two-fluid nozzle. The specific surface area of the powders was measured by the BET method using nitrogen adsorption.
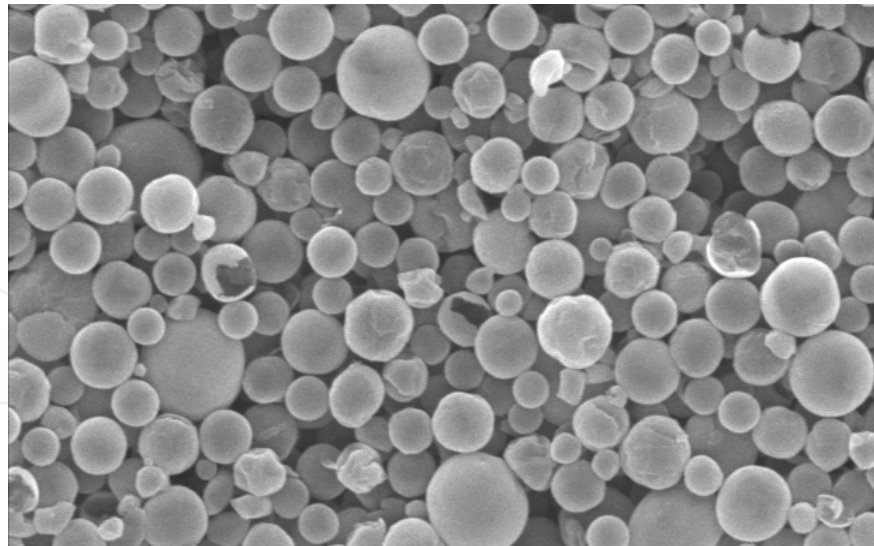
Fig. 2. SEM photograph of LiFePO$_4$/C powders derived from spray pyrolysis

The specific surface area of the LiFePO$_4$/C powders was approximately 10 m²/g regardless of the type of carbon sources used; this suggests that the particle microstructure of LiFePO$_4$/C powders was porous. The particle densities of the LiFePO$_4$/C powders obtained from sucrose and citric acid were 3.5 kg/m³ and 3.2 kg/m³, respectively. It was considered that the hollow or porous microstructure led to a reduced particle density of the LiFePO$_4$/C powders.

3.3 Electrochemical properties of LiFePO$_4$/C cathode materials

Figure 3 shows the rechargeable curves of LiFePO$_4$ and LiFePO$_4$/C cathodes at 1C. The long plateau was observed at about 3.5 V in the rechargeable curves. The discharge capacity of carbon-free LiFePO$_4$ cathode was about 20 mAh/g because of the poor electrical conductivity. It was found that the rechargeable capacity of LiFePO$_4$ was considerably improved by the addition of carbon. The discharge capacity of LiFePO$_4$/C cathode derived from citric acid exhibited 150 mAh/g. That of LiFePO$_4$/C cathode derived from sucrose exhibited 149 mAh/g.
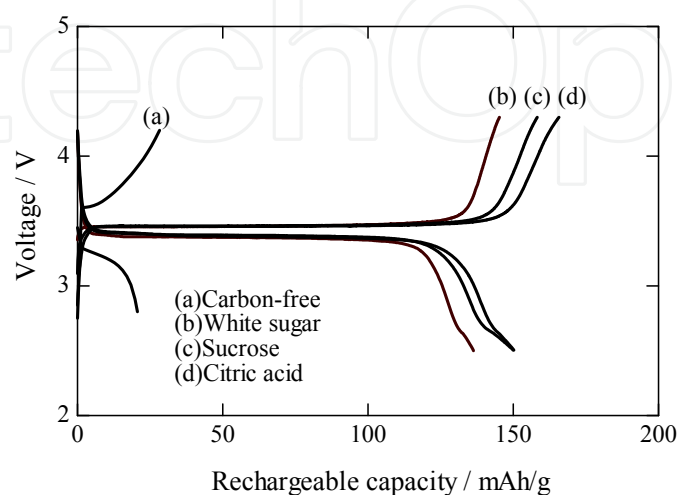

Fig. 3. Rechargeable curves of LiFePO$_4$ and LiFePO$_4$/C cathodes at 1 C

The discharge capacity of $LiFePO_4/C$ cathode derived from other organic compound such as fructose, white sugar also exhibited 136 mAh/g. The rechargeable capacity of $LiFePO_4/C$ cathode derived from citric acid was higher than that derived from sucrose. The carbon content was 2.6 wt% in $LiFePO_4/C$ particles derived from citric acid. The carbon content was 7.1 wt% in $LiFePO_4/C$ particles derived from sucrose. Because the particle size of $C/LiFePO_4$ particles derived from citric acid is close to that of $LiFePO_4/C$ particles derived from sucrose, the excess carbon content (4.5 wt%) may be led to the loss for energy density of $LiFePO_4/C$ cathode derived from sucrose. Figure 4 shows the change of initial discharge capacity of $LiFePO_4/C$ cathode derived from citric acid.
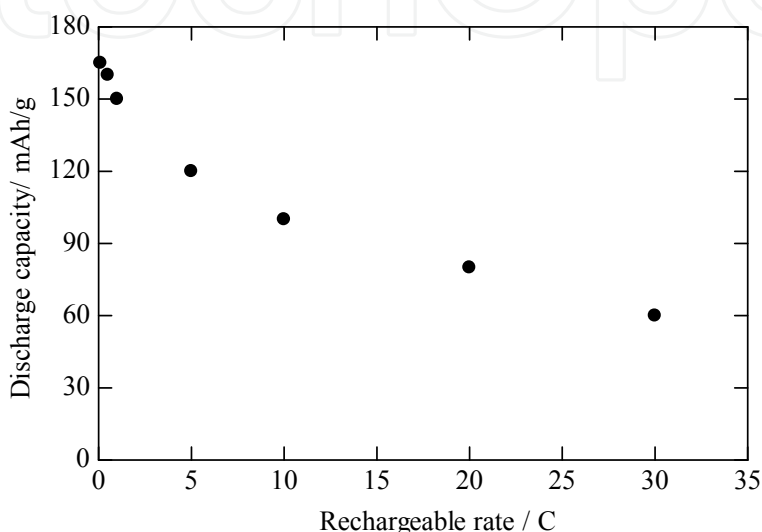
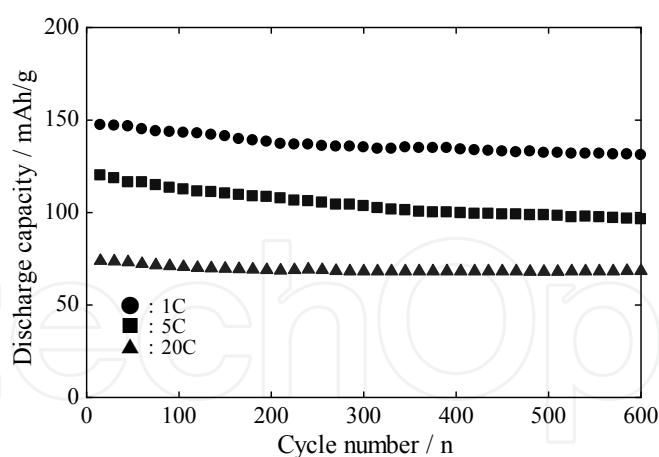Fig. 4. Relation between rechargeable rate and discharge capacity

Fig. 5. Cycle performance of $LiFePO_4/C$ cathode at rechargeable rate indicated

The initial discharge capacity of $LiFePO_4/C$ cathode exhibited 165 mAh/g at 0.1 C. The initial discharge capacity decreased to 100 mAh/g at 10 C. At 30 C, it exhibited 60 mAh/g. Figure 5 shows the relation between cycle number and discharge capacity of $LiFePO_4/C$ cathode derived from citric acid at rate indicated. The cycling was carried out up to 500 cycles. It was clear that $LiFePO_4/C$ cathode had the excellent cycle stability. The discharge capacity of $LiFePO_4/C$ cathode maintained 84 % of initial discharge capacity after 600 cycles at rate of 1 C. The same tendency of cycle stability was also observed in the cycle data at rate of 5 C. The

discharge capacity of LiFePO$_4$/C cathode maintained 94 % of initial discharge capacity after 600 cycles at 20 C. Figure 6 shows the relation between cycle number and discharge capacity of LiFePO$_4$/C cathode at 50 °C. The rechargeable test of coin cell was examined up to 100 cycles at rate of 1C. The coin cell was heated on the hot plate which was kept to 50 °C. The discharge capacity of LiFePO$_4$/C cathode derived from citric acid exhibited 147 mAh/g and the cycle life of it was also stable. The discharge capacity of LiFePO$_4$/C cathode maintained 96 % of initial discharge capacity after 100 cycles. It was found that LiFePO$_4$/C cathode had high cycle stability at the elevated temperature.
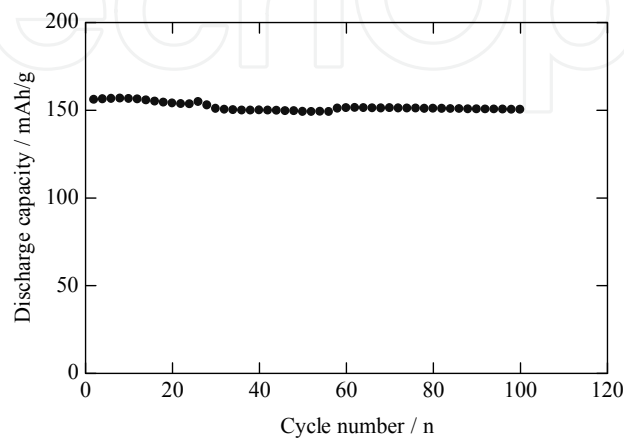
Fig. 6. Cycle performance of LiFePO$_4$/C cathode at 50 °C

4. Li$_4$Ti$_5$O$_{12}$/C anode materials

Various types carbons (Ohzuku, et.al, 1993, Ozawa et.al, 1994, Endo, et.al, 1996, Qiu, et.al, 1996, Buiel, et.al, 1999, Matsumura, et.al, 1995) have been always used as an anode material because they has better safety characteristic and long cycle life compared with lithium metal. It was well known that the carbon anode leads to the formation of dendrite at high rate charging. The solid electrolyte interface (SEI) layer on the carbon anode, which is usually formed at the potential below 0.8 V and accompanied over time with active lithium loss, an increase in impedance, a decrease in rechargeable capacity and fade in cycle life of lithium ion batteries. For an application of EVs and HVs, the oxide type anode is also expected as the candidate for anode materials because of better safety. Spinel type Li$_4$Ti$_5$O$_{12}$ has been demonstrated as an alternative anode material because it has a long plateau at 1.5 V and exhibited excellent cycle life due to the structure stability for the intercalation of Li ion. The disadvantage of Li$_4$Ti$_5$O$_{12}$ for anode was low electronic conductivity because Li$_4$Ti$_5$O$_{12}$ was ionic crystal with insulation. To improve the electric conductivity of it, the foreign metals with various valence numbers (Kubiak, et.al, 2003, Chen, et.al, 2001, Robertson, et.al, 1999, Mukai, et.al, 2005, Huang, et.al, 2006) or the carbon is added to Li$_4$Ti$_5$O$_{12}$ powders. Especially, many researchers have been reported that the addition of carbon is effective for the improvement of electrochemical properties (Gao, et.al, 2007, Huanga, et.al, 2006, Hao, et.al, 2007). So far, it was well known that the solution techniques such as spray drying, sol-gel enabled to homogeneously dope the carbon to Li$_4$Ti$_5$O$_{12}$/C powders (Gao, et.al, 2006, Hao, et.al, 2006, Hao, et.al, 2005). Ju et al applied the spray pyrolysis to the preparation of Li$_4$Ti$_5$O$_{12}$/C anode powders. They have been reported that Li$_4$Ti$_5$O$_{12}$/C powders derived from spray pyrolysis exhibits higher rechargeable capacity and good cycle performance (Yang, et.al, 2006, Ju, et.al, 2009).

4.1 Preparation of Li₄Ti₅O₁₂/C anode materials

Titanium tetraisoproxide (Ti(iso-OC$_3$H$_7$)$_4$, denoted as TTIP) and LiNO$_3$ were used as raw materials. They were dissolved in an atomic molar ratio of Li/Ti to prepare the starting aqueous solution. Organic compound as a carbon source was also added to starting solution. The concentration of starting solution ranged from 0.1 to 1 mol/dm³. The concentration of organic compound was ranged from 0.1 to 0.4 mol/dm³. Lactic acid, malic acid, citric acid and malonic acid were used as an organic compound. The mist of starting solution prepared was generated with an ultrasonic vibrator (1.6 MHz) and introduced into quartz tube (38 mmϕ × 2000 mm) in the electrical furnace with air carrier (6 dm³/min). The mist was drying at 400 °C and then decomposed at 700 °C. The temperatures of electrical furnaces that were used to dry and pyrolysis were set to 400 °C and 700 °C, respectively. As-prepared Li₄Ti₅O₁₂/C particles were continuously collected using the bag filter.

4.2 Preparation of Li₄Ti₅O₁₂/C anode materials

Figure 7 shows typical SEM photograph and particle size distribution of as-prepared Li₄Ti₅O₁₂/C powders formed by spray pyrolysis. SEM photograph reveal that as-prepared particles have spherical morphology with non-aggregation and that the microstructure is dense. No particles with irregular morphology or hollow microstructure were observed.
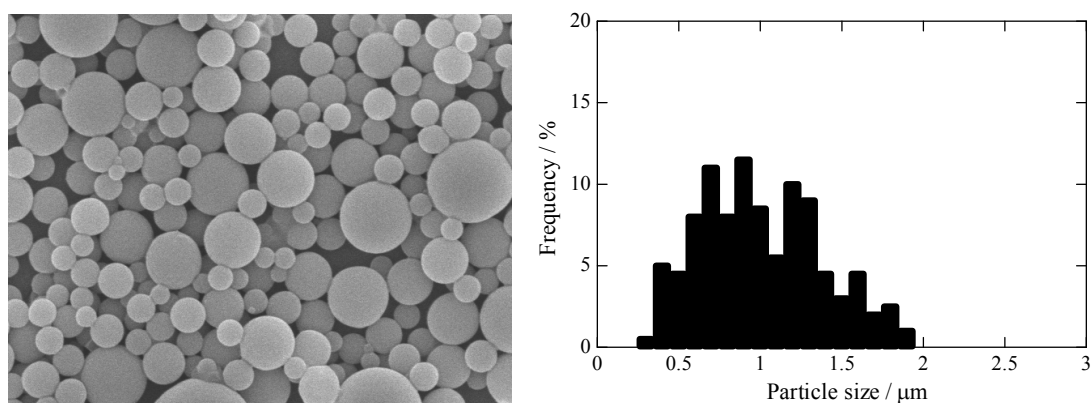

Fig. 7. SEM photograph and particle size distribution of Li₄Ti₅O₁₂/C powders derived from spray pyrolysis

The particle size of as-prepared powders was about 1 μm. SEM photograph also indicate that the as-prepared particles had a broad size distribution. The particle size of all samples ranged from 300 nm to 2000 nm. The geometrical standard deviation (σ_g) of the as-prepared particles was 1.4. Table 1 summarizes the physical properties of Li₄Ti₅O₁₂/C powders derived from various types of organic acids.

Type of acid	Particle size (nm)	Size distribution (P_g)	Atomic ratio Li/Ti ratio[a]	SSA (m²/g)[a]	SSA (m²/g)[b]	Crystal phase[b]	Lattice constant (nm)
Lactic acid	990	1.41	4:5	54.0	24.0	Spinel	0.8358
Citric acid	996	1.41	4:5	51.3	24.7	Spinel	0.8358
Malic acid	990	1.40	4:5	50.0	24.0	Spinel	0.8358

a : as-prepared

b : calcination at 700°C

Table 1. Physical properties of Li₄Ti₅O₁₂/C powders derived from various types of organic acids

The average particle size and σ_g was independent on the organic acid used. The BET measurement results revealed that as-prepared powders had a high specific surface area that ranged from 50 to 60 m^2/g. This result suggested that as-prepared powders had a porous microstructure that consisted of primary particles. After the calcination at 700 °C, their SSA decreased to about 20 m^2/g and the primary particles were sintered. ICP analysis indicated that the Li/Ti ratio of as-prepared powders was in good agreement with that of the starting solution composition. This suggested that the Li^+ and Ti^{4+} ions were homogeneously blending in each mist; this acted as a microreactor. Figure 8 shows the typical differential thermal analysis-thermal gravimetry (DTA-TG) curves of as-prepared powders obtained from lactic acid. TG curves indicated that the weight loss of as-prepared powders was due to the volatility of carbon. The weight loss was approximately 13 wt%. The exothermic peak corresponding to the volatility of carbon was observed at 460 °C in the DTA curve. It was found that the $Li_4Ti_5O_{12}$ particles had high carbon content. In spray pyrolysis, the residence time of the particles in the electric furnace was less than 30 s. Therefore, because $Li_4Ti_5O_{12}$ particles were collected by a bag filter before the organic acid volatilized, it was considered that the carbon remained in the $Li_4Ti_5O_{12}$ particles.
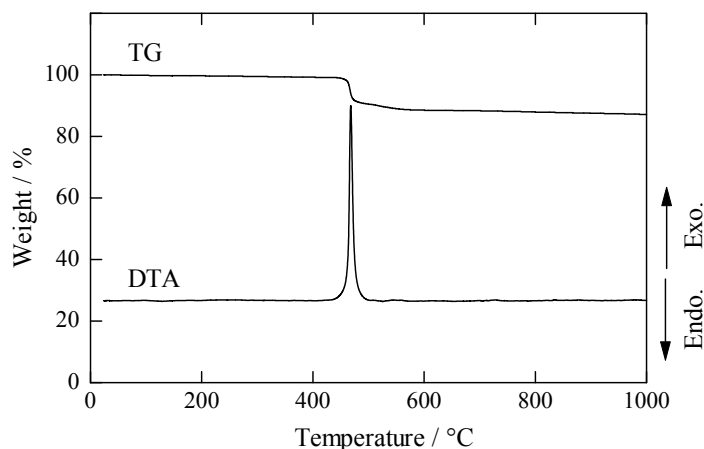

Fig. 8. DTG curve of $Li_4Ti_5O_{12}/C$ powders

Table 2 summarizes the relationship between organic acid and carbon content. The carbon content of $Li_4Ti_5O_{12}/C$ powders obtained from citric acid and malic acid was 11.8 wt% and 10.6 wt%, respectively.

Type of acid	Carbon content (wt%)
Lactic acid	12.8
Citric acid	11.8
Malic acid	10.6

Table 2. Relation between organic acid and carbon content

This suggests that the volatility of carbon from $Li_4Ti_5O_{12}/C$ particles in the pyrolysis process has the following order: malic acid, citric acid, and lactic acid. It is known that carboxylic acid leads to the formation of the Ti^{4+} ion complex compound in the aqueous solution. Kakihana et al. already reported (Kakihana, et.al, 2004) chelating of Ti^{4+} ion by lactic acid in aqueous solution as shown in Fig.9. Therefore, we consider that the Ti^{4+} ion complex

compound in our case was also formed by malic acid and citric acid, because a stable aqueous solution was obtained without the precipitation of titanium hydroxide. Volatilization of carbon is suppressed during the particle formation because of the chemical bonding of the Ti^{4+} ions with lactic acid. Similarly, the volatilization of carbon is suppressed by the chemical bonding of the Ti^{4+} ions with malic acid or citric acid, which is also carboxylic acid of the same type as lactic acid. Figure 10 shows the typical XRD patterns of $Li_4Ti_5O_{12}/C$ powders obtained from lactic acid. The diffraction patterns of all samples were in good agreement with the spinel structure (space group: Fd3m), and other phases were not observed. As-prepared powders were already crystallized to $Li_4Ti_5O_{12}$. It was considered that Li_2O and TiO_2 were rapidly formed in the mist and their solid-state reaction occurred during the pyrolysis. As-prepared powders (a) were calcined in the range of 700 °C (b) to 800 °C (c); powders were well crystallized by the calcination under nitrogen. The lattice constant of calculated $Li_4Ti_5O_{12}$ was a = 0.8358 nm, which is in agreement with the values in the literature (Ohzuku, et.al, 1995).
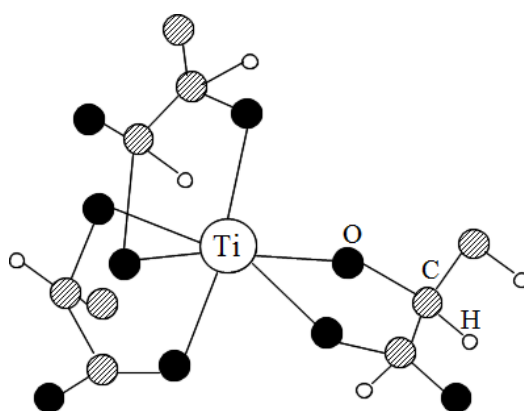

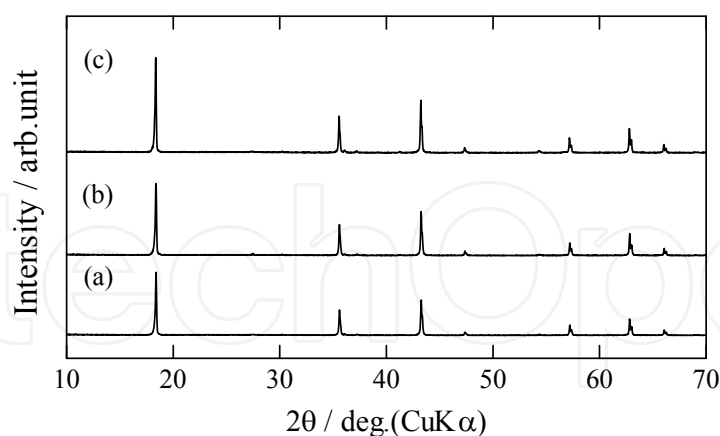Fig. 9. Schematic diagram of Ti complex in the aqueous solution

Fig. 10. XRD patterns of as-prepared $Li_4Ti_5O_{12}/C$ powders a) and $Li_4Ti_5O_{12}/C$ powders calcined at 700 °C b) and 800 °C c)

4.3 Electrochemical properties of Li₄Ti₅O₁₂/C anode materials

Figure 11 shows the rechargeable curves of $Li_4Ti_5O_{12}/C$ anode at 1 C. The long plateaus were observed at 1.5 V in the rechargeable curves. When lactic acid was used as a carbon source, the charge and discharge capacity of the $Li_4Ti_5O_{12}/C$ anode was 170 mAh/g and 165

mAh/g at 1 C, respectively. The efficiency of rechargeable capacity in this case was approximately 97%. These values were higher than those of carbon-coated $Li_4Ti_5O_{12}$ and $Li_4Ti_5O_{12}$/C prepared by spray pyrolysis. $Li_4Ti_5O_{12}$/C anode derived from citric acid exhibited a charge and discharge capacity of 157 mAh/g and 152 mAh/g at 1 C, respectively, and the efficiency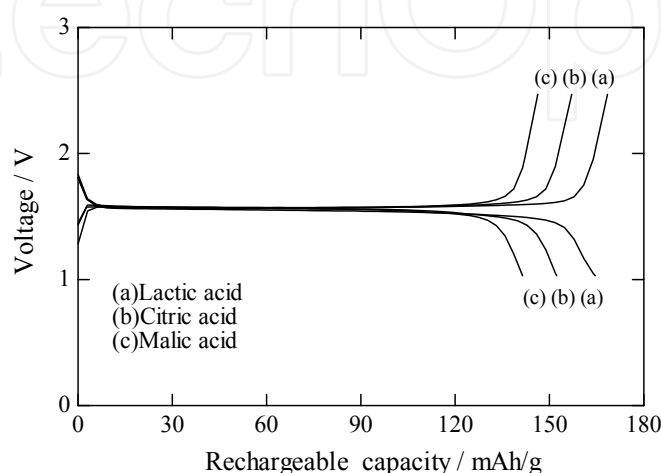 of rechargeable capacity was approximately 97 %. $Li_4Ti_5O_{12}$/C anode derived from citric acid exhibited a charge and discharge capacity of 146 mAh/g and 140 mAh/g at 1 C, respectively, and the efficiency of rechargeable capacity was approximately 96 %.

Fig. 11. Rechargeable curves of $Li_4Ti_5O_{12}$/C anode at 1C

$Li_4Ti_5O_{12}$/C anode derived from lactic acid exhibited the highest capacity and efficiency among all the organic acids used. It was thus confirmed that the rechargeable capacity was affected by the carbon content Figure 12 shows the change in the initial discharge capacity of the $Li_4Ti_5O_{12}$/C anode at the rechargeable rate indicated.
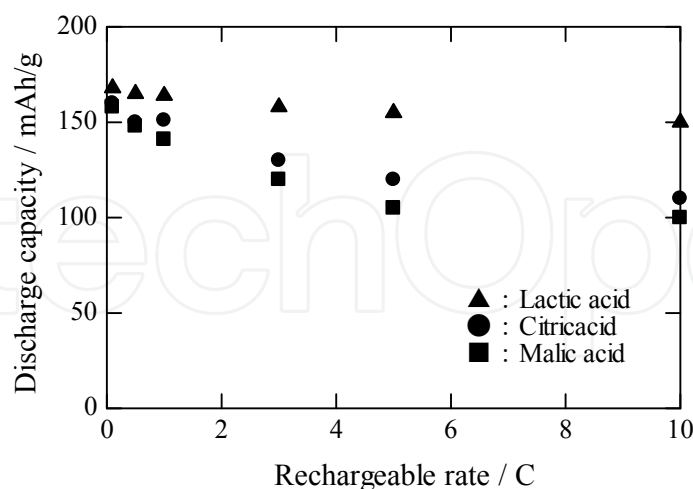

Fig. 12. Rate performance of $Li_4Ti_5O_{12}$/C anode

The initial discharge capacity of the $Li_4Ti_5O_{12}$/C anode gradually decreased with increasing rechargeable rate. The initial discharge capacity of the $Li_4Ti_5O_{12}$/C anode obtained from lactic acid decreased to 150 mAh/g at 10 C. The retention of the initial discharge capacity for 1 C was 91 %. It was found that the $Li_4Ti_5O_{12}$/C anode obtained from lactic acid had a

relatively high discharge performance at a high rechargeable rate, which indicates superior rechargeable performance compared to that of $Li_4Ti_5O_{12}$/C otained by spray pyrolysis and spray drying (Wen, et.al., 2005) and that of carbon-coated $Li_4Ti_5O_{12}$/C (Wang, et.al., 2007). On the other hand, when citric acid and malic acid were used as the carbon source, the initial discharge capacity of the $Li_4Ti_5O_{12}$/C anode decreased to 110 mAh/g and 100 mAh/g at 10 C, respectively. The efficiency in this case for 1 C was 68 % and 63 %, respectively. The rechargeable rate was influenced by the carbon content.
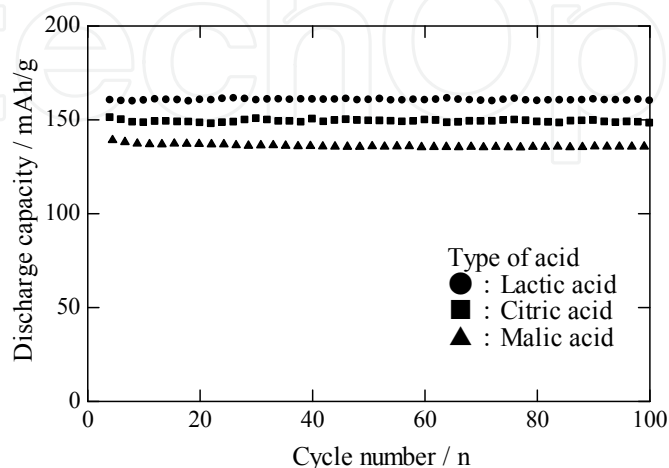

Fig. 13. Cycle performance of $Li_4Ti_5O_{12}$/C anode at 1C
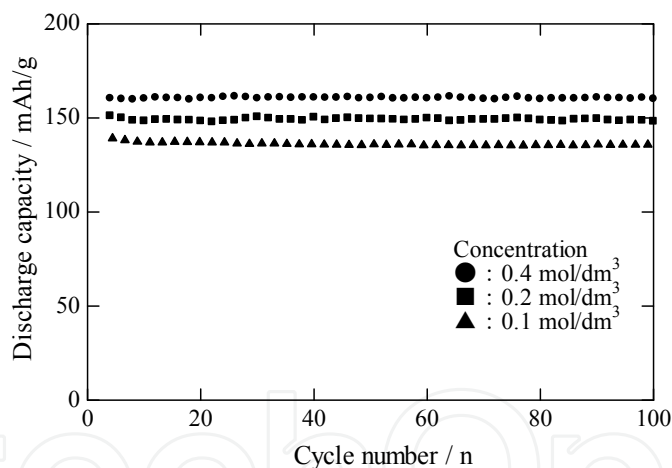

Fig. 14. Cycle performance of $Li_4Ti_5O_{12}$/C anode with different carbon content

Figure 13 shows the relationship between the cycle number and the discharge capacity of the $Li_4Ti_5O_{12}$/C anode at 1 C. The rechargeable test was conducted with up to 100 cycles at room temperature. It was clear that $Li_4Ti_5O_{12}$/C anode had excellent cycle stability regardless of the organic acid type. The discharge capacity of $Li_4Ti_5O_{12}$/C anode obtained from lactic acid maintained 98 % of the initial discharge capacity after 100 cycles at 1 C. When citric acid and malic acid were used, the rechargeable capacity of $Li_4Ti_5O_{12}$/C anode reduced to 150 mAh/g and 138 mAh/g, respectively. The cycle performance showed high stability in the cycle data of both citric acid and malic acid. The retention ratio of the discharge capacity of $Li_4Ti_5O_{12}$/C anode obtained from citric acid and malic acid was 94 % and 96 %, respectively. Figure 14 shows the relationship between the cycle number and the discharge capacity of the $Li_4Ti_5O_{12}$/C anode prepared with different concentration of lactic acid.

The rechargeable rate was 1 C at 25 °C. When the concentration of lactic acid was 0.1 mol/dm^3, the carbon content in the $Li_4Ti_5O_{12}$/C anode was 9 wt% according to TG analysis and the initial discharge capacity of the anode was 141 mAh/g. When the concentration of lactic acid was 0.2 mol/dm^3, the carbon content in the $Li_4Ti_5O_{12}$/C anode was 11 wt% and the initial discharge capacity of the anode was 151 mAh/g. The initial discharge capacity of the $Li_4Ti_5O_{12}$/C anode increased to 162 mAh/g when the concentration of lactic acid was 0.4 mol/dm^3 (12.8 wt%). It was confirmed that the initial discharge capacity increased with increasing carbon content. The retention ratio of the discharge capacity after 100 cycles was more than 95 % for all $Li_4Ti_5O_{12}$/C anodes.

Figure 15 shows the relationship between the cycle number and discharge capacity of $Li_4Ti_5O_{12}$/C anode at 50 °C. The rechargeable test of the coin cell was examined at 1 C for up to 100 cycles while it was heated on the hot plate, which was kept at 50 °C. The discharge capacity of $Li_4Ti_5O_{12}$/C anode derived from lactic acid was 161 mAh/g and its cycle life was stable. The $Li_4Ti_5O_{12}$/C anode maintained 97 % of the initial discharge capacity after 100 cycles. It was found that $Li_4Ti_5O_{12}$/C anode had high cycle stability at an elevated temperature as well as at room temperature. It has been reported (Nakahara, et.al., 2003) that the rechargeable capacity and cycle stability of the $Li_4Ti_5O_{12}$/C anode at 50 °C are superior to those at 25 °C. This may result from the increase in the electric conductivity of $Li_4Ti_5O_{12}$/C at 50 °C.
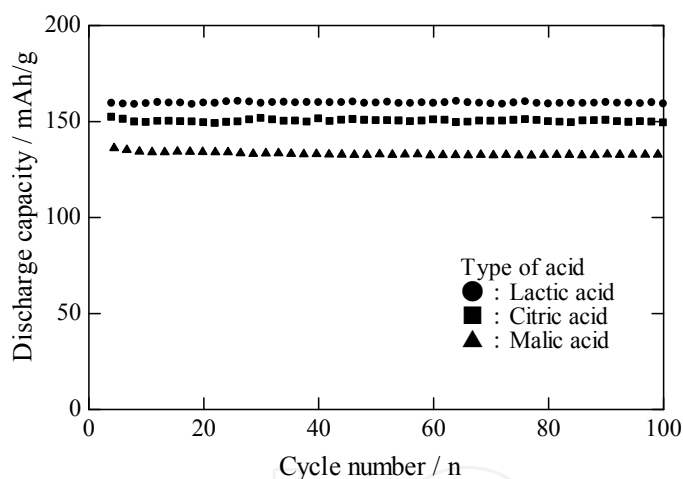

Fig. 15. Cycle performance of $Li_4Ti_5O_{12}$/C anode at 50 °C

5. Conclusions

$LiFePO_4$ cathode and $Li_4Ti_5O_{12}$ anode materials were successfully synthesized by spray pyrolysis using an aqueous solution with an organic acid. They had spherical morphology with a porous microstructure. The as-prepared powders had a high crystallinity with a homogeneous composition. The rechargeable properties of $LiFePO_4$/C cathode and $Li_4Ti_5O_{12}$/C anode were significantly improved by the addition of carbon. The rechargeable capacity of them was also dependent on the carbon content. The discharge capacity of $LiFePO_4$/C cathode and $Li_4Ti_5O_{12}$/C anode was 170 and 165 mAh/g at 1 C, respectively. They had also a high rechargeable capacity at high charging rate and a high retention ratio of rechargeable capacity. The high cycle stability of $LiFePO_4$ cathode and $Li_4Ti_5O_{12}$ anode was also maintained at the elevated temperature. It was concluded that the cathode and anode materials derived from spray pyrolysis were suitable as the electrode for lithium ion battery.

6. References

Aikiyo, H.; Nakane, K., Ogata, N. & Ogihara, T. (2001). *J. Ceram. Soc. Jpn.*, Vol.109, pp.197-200

Barker, J.; Saidi, M.Y. & Swoyer, J.L. (2003). *Electrochem. Solid State Lett.*, Vol.6, pp. A53-55

Bewlay, S.L.; Konstantinov, K., Wang, G.X., Dou, S.X. & Liu, H.K. (2004). *Mater. Lett.*, Vol.58, pp. 1788-1191

Buiel, E. & Dahn, J.R. (1999). *Electrochimi Acta*, Vol.45, pp. 121-130

Chen, C.H.; Vaughey, J.T. & Jansen, A.N. (2001). *J. Electrochem. Soc.*, Vol.148, pp. A102-A104

Dubois, B.; Ruffier, D. & Odier, P. (1989). *J. Am. Ceram. Soc.*, Vol.72, pp. 713-715

Endo, M.; Nishimura, Y., Takahashi, T., Takeuchi, K. & Dresselhaus, M.S. (1996). *J. Phys. Chem. Solids*, Vol.57, pp. 725-728

Gao, J.; Jiang, C., Ying, J. & Wan C. (2006). *J. Power Sources*, Vol.155, pp. 364-367

Gao, J.; Ying, J., Jiang, C. & Wan, C. (2007). *J. Power Sources*, Vol.166, pp. 255-259

Guyomard, D. & Trascon, J.M. (1994). *Solid State Ionics*, Vol.69, pp. 222-237

Hao, Y.; Lai, Q., Lu, J., Wang, H., Chen, Y. & Ji, X.Y. (2006). *J. Power Sources*, Vol.158, pp. 1358-1364

Hao, Y.; Lai, Q., Lua, J., Liu, D. & Ji, X. (2007). *J. Alloys Compd.*, Vol.439, pp. 330-336

Hao, Y.; Lai, Q., Xu, X., Liu, X. & Ji, X.Y. (2005). *Solid State Ionics*, Vol.176, pp. 1201-1206

Huang, S.; Wen, Z., Zhang, J., Gu, Z. & Xu, X. (2006). *Solid State Ionics*, Vol.177, pp. 851-855

Huanga, J. & Jiang, J. (2008). *Electrochimi. Acta*, Vol.53, pp. 7756-7759

Idemoto, Y.; Sekine, H., Ui, K. & Koura, N. (2004). *Electrochemistry*, Vol.70, pp. 564-568

Iida, N.; Nakayama, K., Lenggoro, I.W. & Okuyama, K. (2001). *J. Soc. Powder Technol. Jpn.*, Vol.38, pp. 542-547

Ishizawa, H.; Sakurai, O., Mizutani, N. & Kato, M. (1985). *Yogyo-Kyokai-shi*, Vol.93, pp. 382-386

Ju, S. & Y. Kang, (2009). *J. Phys. Chem. Solids*, Vol.70, pp. 40-44

Kakihana, M.; Tomita, K., Petrykin, V., Toda, M., Sasaki, S. & Nakamura, Y. (2004). *Inorg. Chem.*, Vol.43, pp. 4546-4548

Kubiak, P.; Garcia, A., Womes, M., Aldon, L., Fourcade, J.O., Lpens, P.E. & Jumas, J.C. (2003). *J. Power Sources*, Vol.119–121, pp. 626-630

Markovsky, B.; Talyossef, Y., Salitra, G., Aurbach, D., Kim, H.J. & Choi, S. (2004). *Electrochem.Commun.*, Vol.6, pp. 821-826

Matsumura, Y.; Wang, S., Shinohara, K. & Maeda, T. (1995). *Synthetic*, Vol.71, pp. 1757-1758

Messing, G.L.; Zhang, S.C. & Javanthi, G.V. (1993). *J. Am. Ceram. Soc.*, Vol.76, pp. 2707-2726

Mizushima, K.; Jones, P.C. Wiseman, P.J. & Goodenough, J.B. (1980). *Mat. Res. Bull.*, Vol.15, pp. 783-789

Mukai, K.; Ariyoshi, K. & Ohzuku, T. (2005). *J. Power Sources*, Vol.146, pp. 213-216

Nakahara, K.; Nakajima, R., Matsushima, T. & Majima, H. (2003). *J. Power Sources*, Vol.117, pp. 131-136

Ogihara, T.; Aikiyo, H., Ogata, N. & Mizutani, N. (1999). *Adv. Powder Technol.*, Vol.10, pp. 37-50

Ogihara, T.; Ogata, N., Yonezawa, S., Takashima, M. & Mizutani, N. (1998). *Denki Kagaku*, Vol.66, pp. 1202-1205

Ogihara, T.; Saito, Y., Yanagwa, T., Ogata, N., Yoshida, K., Takashima, M., Yonezawa, S., Mizuno, Y., Nagata, N. & Ogawa, K. (1993). *J. Ceram. Soc. Jpn.*, Vol.101, pp. 1159-1163

Ohzuku, T.; Iwakoshi, Y. & Sawai, K. (1993). *J. Electrochem. Soc.*, Vol.140, pp.2490-2498

Ohzuku, T.; Ueda, A. & Yamamoto, N. (1995). *J. Electrochem. Soc.*, Vol.142, pp. 1431-1435

Ozawa, K. (1994). *Solid State Ionics*, Vol.69, pp. 212-221

Padhi, A.K.; Nanjundaswamy, K.S. & Goodenough, J.B. (1997). *J. Electrochem. Soc.*, Vol.144, pp. 1188-1194

Park, S.H. & Sun, Y.K. (2004). *Electrochimi. Acta*, Vol.50, pp. 431-434

Park, S.H. & Sun, Y.K. (2004). *Electrochimi. Acta*, Vol.50, pp. 431-434

Park, S.H.; Yoon, C.S., Kang, S.G., Kim, H.S., Moon, S.I. & Sun, Y.K. (2004). *Electrochimi. Acta*, Vol.49, pp. 557–563

Pegeng, Z.; Huiqing, F., Yunfei, F., Zhuo, L. & Yongli, D. (2006). *Rare Metals*, Vol.25, pp. 100-104

Pluym, C.T.; Lyons, S.W., Powell, Q.H., Gurav, A.S. & Kodas, T. (1993). *Mater. Res. Bull.*, Vol.28, pp. 369-376

Qiu, W.; Zhou, R., Yang, L. & Liu, Q. (1996). *Solid State Ionics*, Vol.86, pp. 903–906

Robertson, A.D.; Trevino, L., Tukamoto, H. & Irvine, J.T. (1999). *J. Power Sources*, Vol.81-82, pp. 352-357

Roy, D.M.; Neurgaonkar, R.R., O'holleran, T.P. & Roy, R. (1977). *Am. Ceram. Soc. Bull.*, Vol.56, pp. 1023 -1024

Wang, D.; Li, H., Shi, S., Huang, X. & Chen, L. (2005). *Electrochimi. Acta*, Vol.50, pp. 2955-2958

Wang, G.; Gao, J., Fu, L., Zhao, N.H., Wu, Y.P. & Takamura, T. (2007). *J. Power Sources*, Vol.174, pp. 1109–1112

Wen, Z.; Gua, Z., Huanga, S., Yang, J., Lin, Z. & Yamamoto, O. (2005). *J. Power Source*, Vol.146, pp. 670-673

Yang, M.; Tean, T. & Wu, S. (2006). *J. Power Source*, Vol.159, pp. 307-311
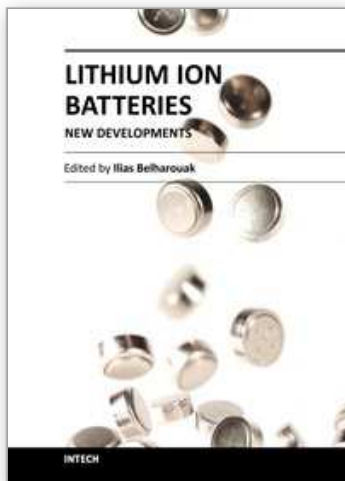
Lithium Ion Batteries - New Developments

Edited by Dr. Ilias Belharouak

The eight chapters in this book cover topics on advanced anode and cathode materials, materials design, materials screening, electrode architectures, diagnostics and materials characterization, and electrode/electrolyte interface characterization for lithium batteries. All these topics were carefully chosen to reflect the most recent advances in the science and technology of rechargeable Li-ion batteries, to provide wide readership with a platform of subjects that will help in the understanding of current technologies, and to shed light on areas of deficiency and to energize prospects for future advances.

How to reference

In order to correctly reference this scholarly work, feel free to copy and paste the following:

Takashi Ogihara (2012). Preparation and Electrochemical Properties of Cathode and Anode Materials for Lithium Ion Battery by Aerosol Process, Lithium Ion Batteries - New Developments, Dr. Ilias Belharouak (Ed.), ISBN: 978-953-51-0077-5, InTech, Available from: http://www.intechopen.com/books/lithium-ion-batteries-new-developments/preparation-and-electrochemical-properties-of-cathode-and-anode-materials-for-lithium-ion-battery-by

INTECH
open science | open minds